Effect of current load on corrosion induced tin whisker growth from SnAgCu solder alloys

Balázs Illés, Tamás Hurtony and Bálint Medgyes

Department of Electronics Technology, Budapest University of Technology and Economics, Budapest, Hungary

billes@ett.bme.hu

Abstract: The effect of current load was investigated on corrosion induced tin whisker growth from SnAgCu (SAC) solder alloys. Three alloys were studied: two low Ag content micro-alloyed SAC and the widely used SAC305. The solder joints were loaded with six different DC current levels between 0–1.5A and they were aged in corrosive environment (85°C/85RH%) for 3000h. The morphology of the whiskers and the micro-structural changes of the solder joints were examined by scanning electron microscope. It was shown that the current load can decrease the corrosion of the solder joints and consequentially it can decrease whiskering as well.

Key words: A. Tin; A. Alloy; B. SEM; C. High temperature corrosion; C. Cathodic protection.

1. Introductions

The tin whiskers are surface deformations of the pure – and in given circumstances alloyed – tin layers [1]. Their usual size is 1-20 μm in diameter and 5-500 μm in length. Tin whisker growth is a serious reliability problem of microelectronics since whiskers result in short circuits between the conducting parts of the electronics like electrochemical migration [2]. Tin whisker formation is caused by the development of mechanical stresses in the tin layer such as: residual stresses of the electroplating; direct mechanical loads; volumetric expansions of the tin layer by intermetallic and oxide layer growth, or temperature change. Whiskers are extruded from the tin layer by a stress release mechanism [1]. Up to 2006, tin-lead alloys (63Sn37Pb and 60Sn40Pb) were mainly used in the electronics industry. The lead was highly effective in restraining tin whisker growth. Transition to lead-free technologies introduced the widespread use of tin-silver-copper (SnAgCu, SAC) solder alloys e.g. 96.5Sn3Ag0.5Cu (SAC305) or 95.5Sn4Ag0.5Cu (SAC405) [3].

The main disadvantage of the lead-free SAC solders is their high price (compared to the leaded alloys) due to their relatively high silver content. Therefore, novel researches aim to reduce the silver content of the SAC solder alloys with retaining the melting temperature between 217–221°C. This can be achieved with micro-alloying other metals (Sb, Bi, Ni, etc.) into the SAC alloys. The new micro-alloyed SAC solders (mSAC) are also called "low silver content SAC solders". In mSAC solder alloys silver content is usually under 1 wt% and the tin content is increased to over 98 wt%. A further aim of the lead-free solder alloy composition researches is to improve the general quality of the solder joints. The 3-4 wt% silver content of the regular SAC alloys might cause the appearance of large amounts of Ag_3Sn intermetallics (IMCs) which are more brittle than the composing metals; these phases might serve as a source of crack initiations [4]. The micro-alloyed metals increase further the mechanical strength of the solder joints [4]. Perevezentsev et al. reached 18% mechanical strength increase with micro-alloying germanium into SAC [5]. Pandher et al. got similar results by micro-alloying of bismuth [6]. Nadia et al. got better wetting ability with adding copper nanoparticles into SAC solders [7].

Besides the previous advantages of the mSAC alloys, they have reliability problems such as tin whisker growth. Skwarek et al. found that commercially used tin-rich alloys Sn/Cu [8] and Sn/Ag/Cu can already develop tin whiskers under thermal shock tests [9, 10], however the length of developed whiskers was only in the range of 10-20 μm which are not dangerous for the microelectronics. Horváth et al. found that high tin content SnCu solder alloys (Cu1-5wt%) can produce tin whiskers under corrosive climate [11]. Chuang et al. observed that alloying 0.5 wt% cerium into the Sn3Ag0.5Cu improves the wetting ability, however, it also stimulates tin whisker growth at an extremely high extent. [12]. Hua et al. observed similar results in the case of same solder alloy doped with In and Zn, where the solder material was corroded in NaCl solution [13]. Marques et al. found whiskers of 30-70 μm in length on SAC solder joints annealed at 125 and 175°C elevated temperatures [14]. However, the number of detected whiskers was not high in the previous studies. Our previous tin whisker research proved that the SAC alloys are more sensitive to corrosive climates than to simple high temperature storage or to thermal shock tests. We found numerous and long (>50μm) tin whiskers with the application of 85°C/85RH% test and it was proven that whisker growth was induced by the corrosion of the solder joints [1]. It was also observed that some mSAC alloys had a bit lower corrosion resistance and consequentially their whiskering ability was a bit higher than in the case of SAC samples [1].

Up to now only a limited number of researches have studied the relation between current load and tin whisker formation. Moreover, the obtained results show contradictions. Brusse et al. found no significant influence of current on tin whisker growth [15] and Hilty et al. observed only minor effects of electric bias on tin whisker growth at room temperature [16]. Nonetheless, some years later it was found that either the high current density [17] or the cycling current pulse [18] in pure tin and the current crowding effect in SAC solders [19] can cause the presence of tin whiskers without any aging condition. He et al. stated that the main responsible factor of filament type whiskers growth from Sn3.8Ag0.7Cu solder joints is the current density accumulation at the crack regions, which leads to higher Joule-heat accumulation that might trigger the whisker formation [20]. Fukuda et al. observed that the application of electrical current slightly reduces whisker density but also slightly increases maximum whisker length [21] and Kim et al. supposed that the current level increases the movement of electrons resulting in the growth of longer whiskers [22]. Consequently, in this research our aim was to study the effect of current load on corrosion induced tin whisker growth from mSAC (and simple SAC) solder alloys.

2. Materials and methods

Three different solder alloys were used in the study: two micro-alloyed Sn based alloys and the most commonly used SAC305. The composition of the alloys can be seen in Table 1 (measured by arc discharge spectroscopy). In order to avoid the influence of the solder flux on the water uptake, and the influence of the acid remnants from the flux on the corrosion properties, the solder pastes were used with the same water base flux. FR4 test board with copper wiring and immersion tin surface finishing was designed for 60 solder joints. The solder pastes were deposited by a stencil printer trough a laser-cut stainless steel stencil with 150 μm thickness [23].

Table 1. Element composition of the studied solder alloys (wt%).

Solder alloy	Sn	Ag	Cu	Bi	Sb
SAC305	96.5	3.0	0.5	–	–
mSAC1	98.4	0.8	0.7	0.1	–
mSAC2	98.9	0.3	0.7	0.1	0.01

The solder joints have fixed copper wires (with 1mm diameter and 3mm length) on the FR4 board. The application of copper wires instead of chip resistors was necessary due to the high current loads and to

avoid the heat dissipation on the components. The copper wires were placed by a semi-automatic pick&place machine. The solder joints were formed in an infrared reflow oven according to the suggested thermal profiles of the different solders. Two test boards were produced from each solder alloys. The 60 solder joints were divided into 6 rows on the FR4 boards according to the applied DC current loads: 0, 0.1, 0.2, 0.5, 1, 1.5A. The test boards were driven with 5 VDC, the different current levels were set with current limiters. The test structure can be seen in Fig. 1. The samples were aged in 85°C/85RH% corrosive climate for 3000 hours.

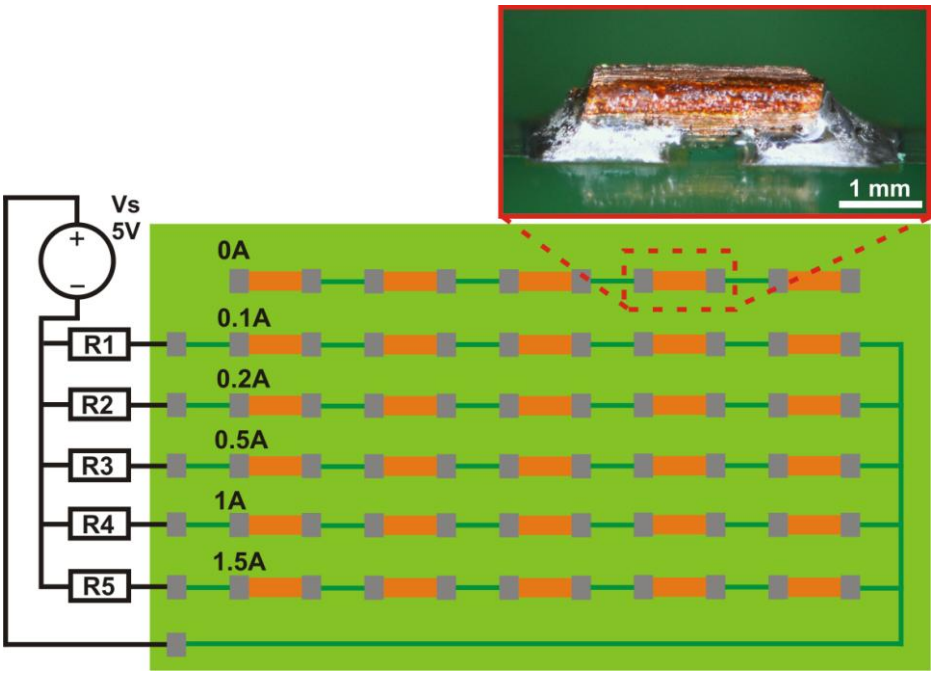

Fig. 1. Schematic of the test structure and a soldered joint.

Whisker growth was monitored at given time checkpoints after every 500 hours by a FEI Inspect S50 Scanning Electron Microscope (SEM), (Acc. Voltage 20 kV). The axial length of a whisker was measured according to the JESD201 standard (means the distance between the tip of the whisker and the surface). The accuracy of the measurement was about ±5 µm. The whisker densities were calculated on SEM micrographs with 1000x magnification. The applied unit of the whisker density was pieces (pcs.)/0.01mm^2. The statistics of the whiskers were calculated from to 25 measurements. The structural changes of the solder joints were observed on cross-sections to study the combined effect of the current load and the corrosive climate. The element composition was measured by a Bruker Energy-dispersive X-ray Spectroscopy (EDS) in SEM.

The cross-sections were treated with two different methods. For the identification of the corroded areas in the solder joints, a special electrochemical etching method [24] was applied. The cross-sections of the solder joints were placed into an electrochemical cell as work electrodes in a standard three electrode measurement setup. In amperometric measurement mode -350mV bias voltage was applied (measured to the Hg-Hg_2Cl_2 reference electrode) to selectively extract the tin phases from the solder joint. Due to the high selectivity only the pure Sn-phases were removed, intermetallic compounds and tin oxide remained intact. By applying this technique the tin oxide was separated from the tin matrix and its spatial structure and material composition became observable. The measurements on the corroded areas were performed by an Olympus BX-51 optical microscope and image analyzer software. A special chemo-mechanical polishing (Oxide Polishing Suspension, OPS) was applied on the cross-section of the samples in order to enhance the optical contrast between regions with different chemical and mechanical properties.

3. Results and discussion

The first tin whiskers have appeared after 1000h aging on all types of solder joints, but only in the case of 0 and 0.1A current levels. Fig. 2 shows the average whisker densities and lengths observed during the test. The *x* axis is not a real quantitative axis; each section shows the coherent results for a time point of the examinations. The scatters in the graphs are the standard deviations. (The relatively high standard deviations of the results are usual in whisker researches.) In the case of the SAC305 samples, the applied current load has got considerable influence on the number of the developed tin whiskers (Fig. 2a)). On the unloaded samples the average whisker density has reached 17.6 pcs/0.01mm^2 at the end of test, while 0.1 A current load has already caused significant decrease in the number of developed whiskers (9.6 pcs./0.01mm^2 at 3000h). In addition, the higher current loads have delayed the appearance of the first tin whiskers. Whiskering was detected only after 1500h in the case of 0.2, 0.5 and 1A; and after 2000h in the case of 1.5A. The whisker density statistics of the current loads between 0.1–1A do not deviate completely from each other (the average whisker densities are between 10.9 and 7.8 pcs./0.01mm^2). However, a clear tendency is visible: higher current loads result in lower amounts of tin whiskers. The results of 1.5A exceed only 5.2pcs./0.01mm^2 average whisker density at 3000h. In the case of the SAC305 samples, considerable influence of the current load on the whisker lengths was not detected (Fig. 2b)). Minor length reduction was observed only on the samples loaded with 0.2 and 1.5A current. The increase of the average length was high after the beginning of

the whiskering (in the first 1500h), which was followed by a moderate linear increase. The average whisker lengths have reached 18.9–22.7 µm at the end of the test.

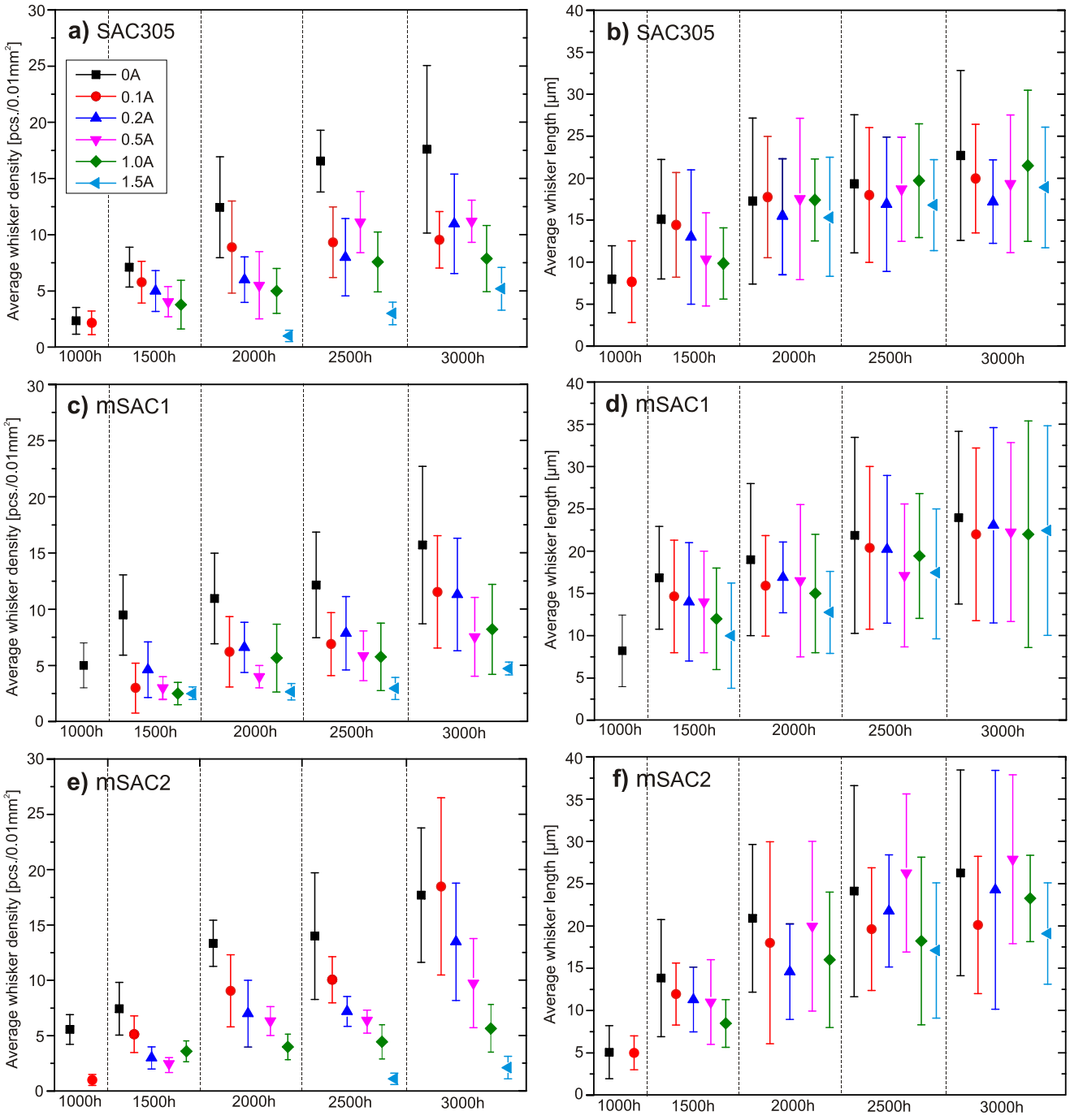

Fig. 2. Whisker statistics of the test: a) average whisker densities on SAC305 solder joints; b) average whisker lengths on SAC305 solder joints; c) average whisker densities on mSAC1 solder joints; d) average whisker lengths on mSAC1 solder joints; e) average whisker densities on mSAC2 solder joints; f) average whisker lengths on mSAC2 solder joints.

In the case of the mSAC1 samples, the positive effect of the current load on the number of the developed tin whiskers is also significant (Fig. 2c)). On the unloaded samples the average whisker density has reached 15.7 pcs/0.01mm^2 while with 1.5A current load it was only 4.8 pcs/0.01mm^2 at the end of test. The results show high similarity to the results of the SAC305 samples (Fig. 2a)), minor difference is that the 0.1A current load has also delayed the whiskering. The average whisker length results of the mSAC1 samples (Fig. 2d)) are also similar to the results of the SAC305 samples (Fig. 2b)). The current load has no considerable effect on the lengths of the tin whiskers. On the mSAC1 joints the average whisker lengths have reached 19.1–23.9 μm at end of the test.

The current load has decreased the number of the developed tin whisker the most consequently on the mSAC2 samples (Fig. 2e)). Only exception is the 0.1A at 3000h. The whisker density statistics of the different current levels are separated. At 0.1A current load the average whisker density was 18.5 pcs/0.01mm^2 while with 1.5A load it was only 2.4 pcs/0.01mm^2 at 3000h. Here the 0.1A current load has not delayed the whiskering but in the case of 1.5A the whiskering was detected only at 2500h. The average whisker length results of the mSAC2 samples (Fig. 2f)) are not as coherent as they are in the case of SAC305 and mSAC1 (Fig. 2b) and 2d)), e.g. the 0.1A load has induced some average length decrease but the 0.5A load performed a bit worse than the unloaded samples. On the mSAC2 samples the average whisker lengths were between 20.1–27.9 μm at the end of the test.

From the aspect of microelectronics reliability, the maximum whisker lengths are also important due to the possible short circuit formation. Table 2 presents the detected maximum tin whisker lengths at the different checkpoints. The maximum whisker length was 192μm on the mSAC2 sample at 3000h, 4 whiskers were longer than 150μm, and more than 30 whiskers were longer than 100μm in the observed surface regions. The longest whiskers were usually detected in the unloaded or low current cases. By nowadays the decrease of the insulation distance in microelectronics has reached the 100μm and it is still continuing [23]. Therefore the probability of short formation by SAC solder whiskers cannot be neglected.

Table 2. The detected maximum tin whisker lengths during the test.

Time [h]	Max. length [µm] (current load)		
	SAC305	**mSAC1**	**mSAC2**
1000	14 (0A)	21 (1A)	17 (0A)
1500	60 (0.2A)	46 (0A)	56 (0.1A)
2000	101 (0A)	105 (0A)	152 (0A)
2500	72 (0.2A)	91 (0A)	161 (0A)
3000	111 (0.1A)	170 (0A)	**192 (0A)**

The observed whiskering behavior of the studied solder alloys accord with the results of our previous study [1]. The mSAC2 alloy has produced the most and longest tin whiskers, while the mSAC1 and SAC305 alloys have both shown better results. The SAC305 alloy has grown a bit more but shorter whiskers than the mSAC1. The type of the developed whiskers was usually nodule due to the diffusion of contaminant atoms (Cu, Bi, Ag) into the whiskers (see more details in [1] and [26]), but this time more filament whiskers were also detected (Fig. 3.). Fig. 4 shows a qualitative effect of the current load on the whisker density. Without current load the 3000h aging has formed hundreds of whiskers on the SAC305 sample, the sample with 0.5A load has significantly less whisker, while the sample with 1.5A load is almost whisker free.

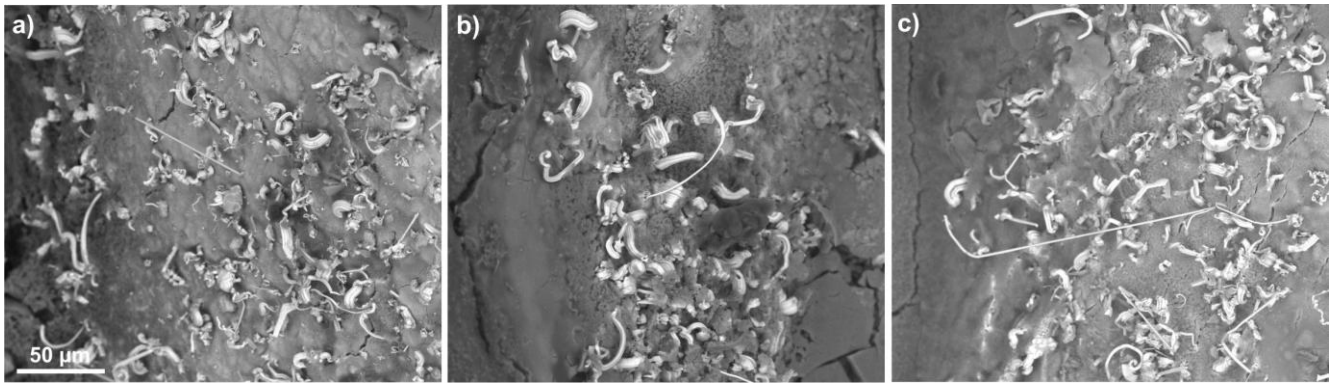

Fig. 3. SEM micrograph of filament and nodule type whiskers at 3000h with 0A current load: a) on SAC305 sample; b) on mSAC1 sample; c) on mSAC2 sample.

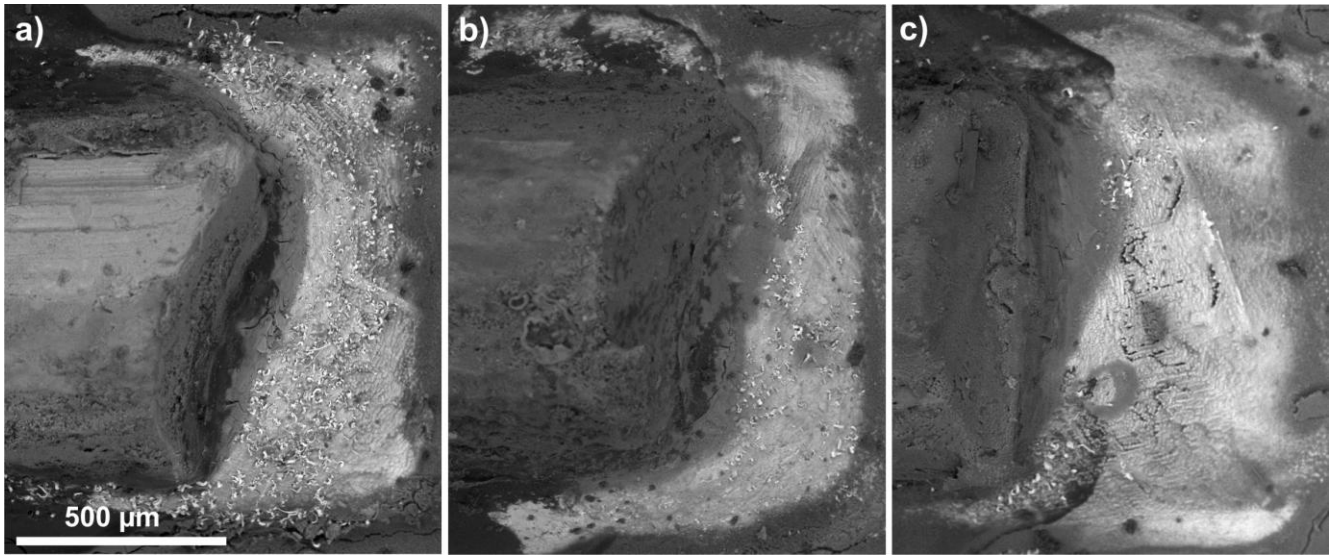

Fig. 4. SEM micrograph of SAC305 solder joints at 3000h: a) an unloaded joint; b) fewer whiskers on solder joint with 0.5A current load; c) an almost whisker free joint with 1.5A current load.

In our previous study it was proven that corrosion is the main indicator of tin whisker growth from the SAC solder alloys, and the whiskering differences between the alloys are caused by the different corrosion resistance of the alloys [1]. The Pilling-Bedworth Ratio (PBR, which gives the volume expansion during a metal oxide formation) for SnO_2 and SnO on pure tin is 1.31 and 1.26, respectively [25]. This means that the corroded tin grains suffer considerable volume expansion that is causing considerable mechanical stress on the neighbouring tin grains which are relaxing this stress by whisker growth. The application of the current load has not changed the whiskering differences between the alloys but it has considerably reduced the number of developed whiskers on all of the samples. Therefore our aim was to find a relation between the current load and the corrosion behavior of the samples. For this purpose, the solder joints were cross-sectioned.

In the first step, an electrochemical etching was applied on some of the cross-sections to identify the corroded areas in the solder joints. In this way, the tin oxide was separated from the tin matrix and its spatial structure and material composition has become observable. Fig. 5 shows an example for the microstructure of an electrochemically etched SAC305 solder joint (1A at 3000h). The etching has left the intermetallics (IMC) and the tin oxides intact. According to the material composition (Tab. 3), the surface of the meniscus of the solder joint is almost totally corroded. The corrosion has penetrated 10-40 µm deep into the solder joint. This was typical for all samples. The selective removal of the pure Sn-phases at the uncorroded areas has increased the relative Ag content at M3 and M4 (Tab. 3).

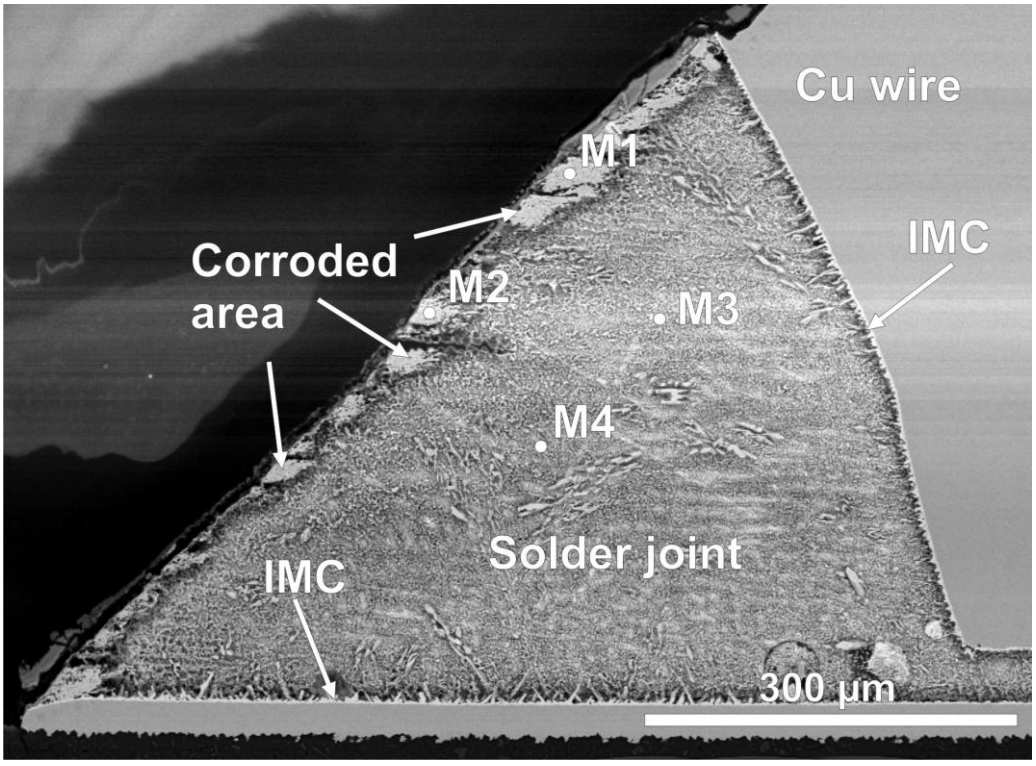

Fig. 5. SEM micrograph of an electrochemically etched SAC305 solder joint, 1A current load at 3000h.

Table 3. Element composition of the SAC305 solder joint in Fig. 5.

Element	M1 [at%]	M2 [at%]	M3 [at%]	M4 [at%]
Sn	22.17	21.91	15.89	12.95
O	***57.80***	***56.57***	24.26	28.81
Ag	1.50	1.28	16.19	13.00
Cu	0.45	0.14	0.89	1.15
C	17.95	20.07	41.92	42.33

In the second step OPS polishing was applied on the rest of the cross-sections to enhance the optical contrast between regions with different chemical and mechanical properties, before the measurement of the corrosion depth in the solder joints. Fig 6 shows an example for the mSAC1 solder joints after the OPS polishing. It is clearly visible that the increasing current load has caused the decrease of corroded areas.

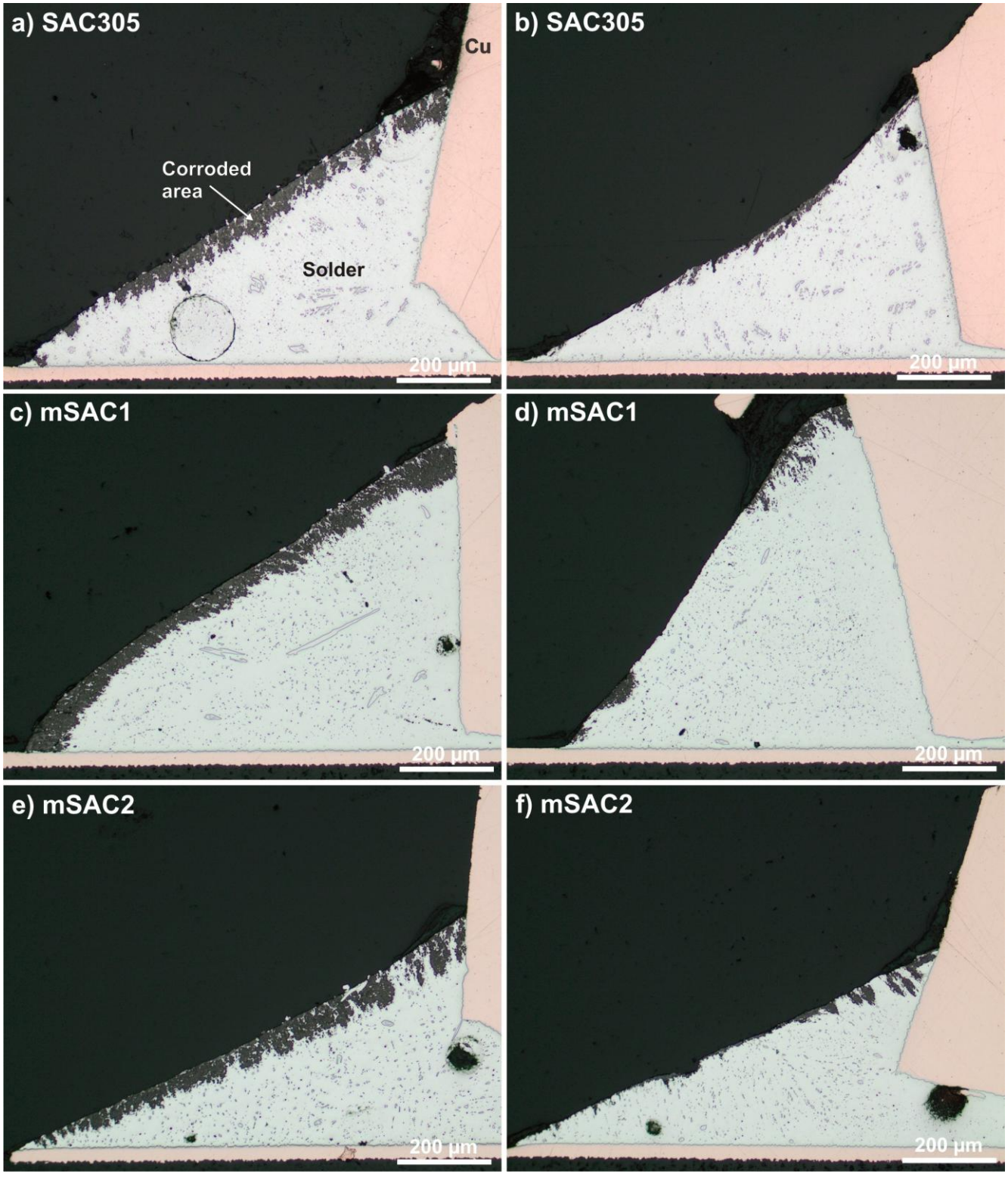

Fig. 6. Optical microscopic images of cross-sectioned solder joints at 3000h: a) SAC305 with 0A current load; b) SAC305 with 1.5A current load; c) mSAC1 with 0A current load; d) mSAC1 with 1.5A current load; e) mSAC2 with 0A current load; f) mSAC2 with 1.5A current load.

For the quantitative analysis of the corrosion level, a novel parameter named spatial corrosion depth (d_{sc}) was introduced. The spatial corrosion depth means the average corrosion depth weighted with the ratio of the corroded length and the length of the solder meniscus:

$$d_{sc} = \bar{d} \cdot \frac{\sum l_i}{L} = \frac{\sum A_i}{\sum l_i} \cdot \frac{\sum l_i}{L} = \frac{\sum A_i}{L} \qquad [\mu m] \tag{1}$$

where $\bar{d}$ is the average corrosion depth, A_i is the area of a corrosion spot, l_i is the length of a corrosion spot on the meniscus and L is the length of the solder meniscus (see in Fig. 7). Practically, the spatial corrosion depth was calculated from the total sum of the corroded areas divided with the length of the meniscus (according to the derivation id Eq.1).

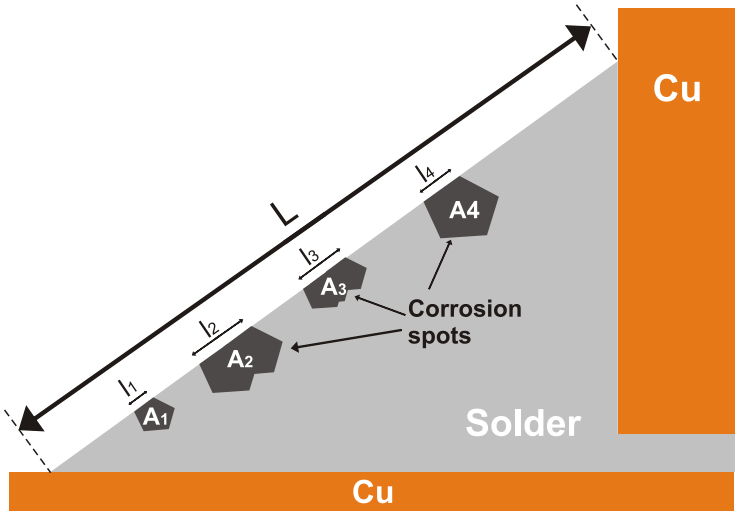

Fig. 7. The variables and the calculation method of the spatial corrosion depth.

This factor is more informative than the simple average corrosion depth since from the point of the whisker growth, not only the corrosion depth is important but the frequency of occurrence of the corroded areas as well. In addition, the spatial corrosion depth shows very low variation in a given solder joint.

The d_{sc} values can be seen in Fig. 8. The *x* axis is not a real quantitative axis; each section shows the coherent results for a current load. The increase of the current load decreases the spatial corrosion depth which results in lower mechanical stress in the upper region of the solder joints and finally results in reduced amount of tin whiskers. The spatial corrosion depth is in good correlation with the average whisker density. The mSAC1 and mSAC2 have a bit higher d_{sc} values (and also a bit higher

average whisker densities) than the SAC305. This quantitative comparison also confirms our previous qualitative comparison about the corrosion behavior of these solder alloys [1].

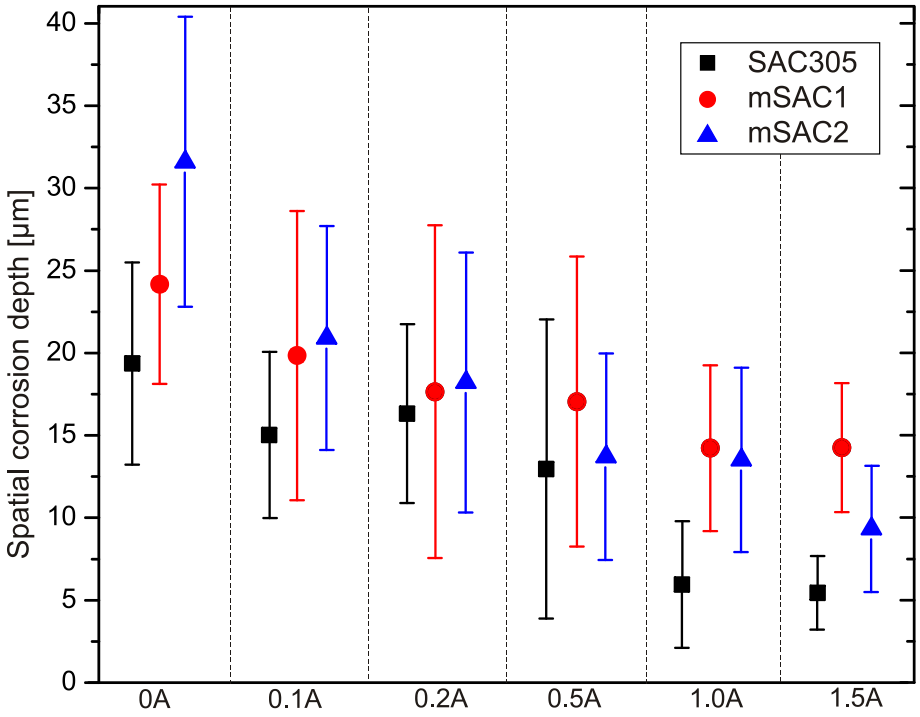

Fig. 8. The spatial corrosion depth of the solder joints at different current loads.

In the case of unbiased samples a galvanic cell is formed between the SAC solder (represented as Sn) and Cu due to the electrode potential difference according to the Nernst equation [27]. In the galvanic cell the effect of cathodic protection [28, 29] is present where Sn is the sacrificial anode and Cu is cathode (Fig. 9).

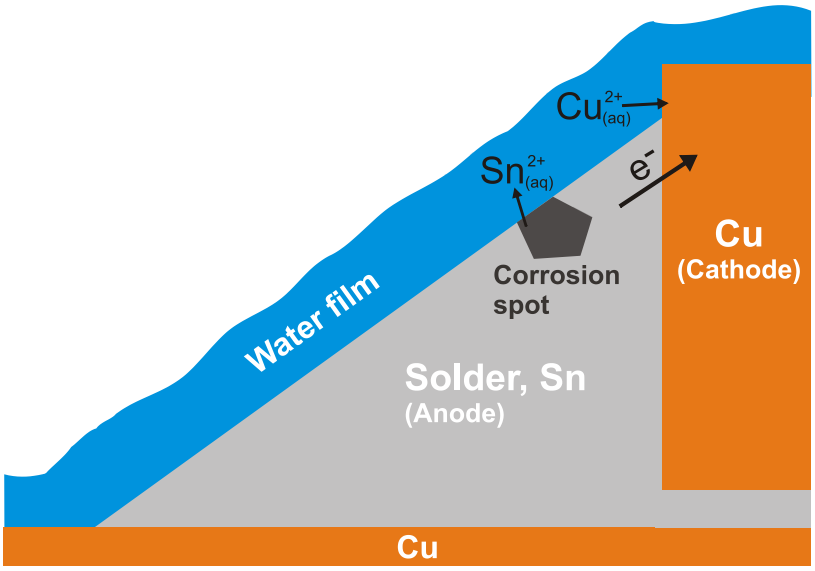

Fig. 9. The formed galvanic cell in the solder joints between the Sn and the Cu.

The Sn electrode (anode) is providing the electrons for the reduction of the cathode which results in rapid corrosion of the upper region of the solder joints. In the case of the biased samples, the current load is also providing electrons for the reduction processes at the cathode. Therefore the oxidation process will be slower at the anode and thus the corrosion mechanism produces smaller amount of oxide at the upper region of the solder joints compared to the unbiased cases (Fig. 8). The previous theory is also supported by the cross-sections in Fig. 6, where minor traces of corrosion can be found on the Cu (cathode) [30]. The effect of the Joule heating on the previously discussed corrosion mechanism could be neglected, since the maximum heating power of the soldered copper wires was in µW range (in the case of 1.5A current load). This very small heating power can not cause any further, considerable temperature changes in a 85°C/85RH% environment, where the heat transfer coefficient of the surrounding medium is extremely high.

5. Conclusions

In this study, the effect of current load was investigated on corrosion induced tin whiskering growth from lead-free Sn/Ag/Cu (SAC) solder alloys. It was proven that the corrosion climate can effectively indicate tin whisker growth by the corrosion of the solder joints. The mSAC2 alloy has produced the highest amount and longest tin whiskers, while the mSAC1 and SAC305 alloys have shown similar and better results. The type of the developed whiskers was usually nodule, but lots of filament-like whiskers were also detected. The increase of the current load has decreased the spatial corrosion depth,

which resulted in lower mechanical stress in the upper region of the solder joints and finally decreased the number of tin whiskers considerably. The decrease of the spatial corrosion depth due to the current load can probably be explained by the following: in the case of biased samples the applied voltage source is also providing electrons for the reduction processes at Cu cathode. Therefore the oxidation will be slower at the Sn anode and thus the corrosion mechanism produces a relatively thinner oxide layer at the upper region of the solder joints compared to the unbiased cases. However, the current load has not shown considerable influence on the whisker lengths. The longest whisker was 192μm on the mSAC2 sample and more than 30 whiskers were longer than 100μm – these cases were usually detected in the unloaded or low current cases. Therefore, the probability of short circuit failure effect generated by SAC solder whiskers cannot be neglected.

6. Acknowledgement

The research leading to these results has received funding from the ProProgressio foundation.

References

[1] B. Illés, B. Horváth, Tin Whisker Growth from Micro-alloyed SAC Solders in Corrosive Climate, J. Alloys Comp. 616 (2014) 116–121.

[2] X. Zhong, G. Zhang, X. Guo, The effect of electrolyte layer thickness on electrochemical migration of tin, Corros. Sci. (2015), in press, DOI: 10.1016/j.corsci.2015.04.014

[3] B. Medgyes, B. Horváth, B. Illés, T. Shinohara, A. Tahara, G. Harsányi, O. Krammer, Microstructure and elemental composition of electrochemically formed dendrites on lead-free micro-alloyed low Ag solder alloys used in electronics, Corros. Sci. 92 (2015) 43–47.

[4] O. Krammer, T. Garami, Reliability Investigation of Low Silver Content Micro-alloyed SAC Solders, Proceedings of 35th International Spring Seminar on Electronics Technology, 2012, pp. 149-154.

[5] B. N. Perevezentsev, M. N. Kurmaev, Microalloying of Alloys of the Sn – Ag – Cu System, Metal Sci. Heat Treat. 11-12 (2009) 540–543.

[6] R. S. Pandher, B. G. Lewis, R. Vangaveti, B. Singh, Drop Shock Reliability of Lead-Free Alloys - Effect of Micro-Additives, Proceedings of Electronic Components and Technology Conference, 2007, pp. 669–676.

[7] A. Nadia, A.S.M.A. Haseeb, Understanding the Effects of Addition of Copper Nanoparticles to Sn-3.5 Ag Solder, Sold. Surf. Mount. Tech. 23/2 (2011) 68–74.

[8] A. Skwarek, J. Ratajczak, A. Czerwinski, K. Witek, J. Kulawik, Effect of Cu addition on whisker formation in tin-rich solder alloys under thermal shock stress, Appl. Surf. Sci. 255 (2009) 7100–7103.

[9] A. Skwarek, K. Witek, J. Ratajczak, Risk of whiskers formation on the surface of commercially available tin-rich alloys under thermal shocks, Microelectron. Reliab. 49 (2009) 569–572.

[10] A. Skwarek, M. Pluska, J. Ratajczak, A. Czerwinski, K. Witeka D. Szwagierczak, Analysis of tin whisker growth on lead-free alloys with Ni presence under thermal shock stress, Mater. Sci. Eng. B 176 (2011) 352–357

[11] B. Horváth, T. Shinohara, B. Illés, Corrosion Properties of Tin-Copper Alloy Coatings in Aspect of Tin Whisker Growth, J. Alloys Compd. 577 (2013) 439-444.

[12] T.-H. Chuang, C.-C. Chi, Effect of adding Ge on rapid whisker growth of Sn–3Ag–0.5Cu–0.5Ce alloy, J. Alloys Compd. 480 (2009) 974-980.

[13] L. Hua, C. Yang, Corrosion behavior, whisker growth, and electrochemical migration of Sn–3.0Ag–0.5Cu solder doping with In and Zn in NaCl solution, Microelectron. Reliab. 51 (2011) 2274–2283.

[14] V.M.F. Marques, C. Johnston, P.S. Grant, Microstructural evolution at Cu/Sn–Ag–Cu/Cu and Cu/Sn–Ag–Cu/Ni–Au ball grid array interfaces during thermal ageing, J. Alloys Comp. 613 (2014) 387–394.

[15] J.A. Brusse, G.J. Eweel, J.P. Siplon, Tin Whiskers: Attributes and Mitigation, Proceeding of 22nd capacitor and resistor technology symposium, 2002, pp. 67–80.

[16] R.D. Hilty, N.E. Corman, H. Herrmann, Electrostatic Fields and Current-Flow Impact on Whisker Growth, IEEE Trans. Electron. Packag. Manuf. 28 (2005) 75-84.

[17] S.H. Liu, C. Chen, P.C. Liu, T. Chou, Tin whisker growth driven by electrical currents, J. Appl. Phys. 95, 7742 (2004).

[18] B. Jiang, A.-P. Xian, Tin whisker growth under cycling current pulse, Conference on High Density Microsystem Design and Packaging and Component Failure Analysis, 2006, pp. 280-284.

[19] F.-Y. Ouyang, K. Chen, K.N. Tu, Y.-S. Lai, Effect of current crowding on whisker growth at the anode in flip chip solder joints, Appl. Phys. Lett. 91, 231919 (2007).

[20] H. He, L. Cao, H. Hao, L. Ma, F. Guo, Whisker growth in the crack region of the cathode interface during current stressing process in leadfree solder joints, 15th International Conference on Electronic Packaging Technology, 2014, pp. 1491-1494.

[21] Y. Fukuda, M. Osterman, M. Pecht, The impact of electrical current, mechanical bending, and thermal annealing on tin whisker growth, Microelectron. Reliab. 47 (2007) 88–92.

[22] K.-S. Kim, J.-M. Yang, J.-P. Ahn, The effect of electric current and surface oxidization on the growth of Sn whiskers, App. Surf. Sci. 256 (2010) 7166–7174.

[23] O. Krammer, L.M. Molnár, L. Jakab, A. Szabó, Modelling the effect of uneven PWB surface on stencil bending during stencil printing process, Microelectron. Reliab. 52/1 (2012) 235-240.

[24] T. Hurtony, A. Bonyár, P. Gordon, G. Harsányi, Investigation of intermetallic compounds (IMCs) in electrochemically stripped solder joints with SEM, Microelectron. Reliab. 52/6 (2012) 1138–1142.

[25] S. D. Cramer, B. S. Covino, ASM Handbook, Volume 13A Corrosion: Fundamentals, Testing, and Protection, Ohio, 2003.

[26] B. Horváth, Influence of copper diffusion on the shape of whiskers grown on bright tin layers, Microelectron. Reliab. 53 (2013) 1009-1020.

[27] W. Sun, L. Wang, T. Wu, G. Liu, An arbitrary Lagrangian–Eulerian model for modelling the time-dependent evolution of crevice corrosion, Corros. Sci. 78 (2014) 233–243.

[28] J. Carmona, P. Garcés, M.A. Climent, Efficiency of a conductive cement-based anodic system for the application of cathodic protection, cathodic prevention and electrochemical chloride extraction to control corrosion in reinforced concrete structures, Corros. Sci., (2015), in press, DOI: 10.1016/j.corsci.2015.04.012

[29] Ph. Refait, M. Jeannin, R. Sabot, H. Antony, S. Pineau, Corrosion and cathodic protection of carbon steel in the tidal zone: Products, mechanisms and kinetics, Corros. Sci. 90 (2015) 375–382.

[30] H. Huang, Z. Pan, X. Gou, Y. Qiu, Effects of direct current electric field on corrosion behaviour of copper, Cl- ion migration behaviour and dendrites growth under thin electrolyte layer, Trans. Nonferrous Met. Soc. China 24 (2014) 285-291.